3-Dimensional Analysis of Flow Patterns and Temperature Profiles for the Growth of InGaSb by Rotational Bridgman Method

T. Ozawa[1], **N. Ishigami**[1], **Y. Hayakawa**[2], **T. Koyama**[2], **M. Kumagawa**[2]

Abstract: To investigate the solution convection in the rotational Bridgman method, both flow patterns and temperature distributions were calculated by solving three equations in 3-dimensional analysis: Navier-Stokes, continuity and energy. We focused on the relationship between ampoule rotational rate and temperature distribution in the growth solution reservoir. In the 3-dimensional model, In-Ga-Sb solution was put between GaSb seed and feed crystals, where seed and feed crystals were cylindrical in shape, and the In-Ga-Sb solution was semi-cylindrical. The ampoule rotational rate was changed in a range of 0 to 100 *rpm*. By increasing the ampoule rotational rate, the flow velocity in the In-Ga-Sb solution increased and the temperature distribution tended to be uniform.

keyword: InGaSb, thermal convection, ampoule rotation, Bridgman method

1 Introduction

Ternary mixed crystals of semiconductors are interesting materials, because fundamental properties such as lattice constant and bandgap energy, can be controlled by adjusting the compositional ratio. The advantage, that mixed crystals offer the possibility to reduce lattice mismatch at the interface between a substrate and an epilayer, has been fully utilized for realization of optical devices. However, it is very difficult to grow large single mixed crystals of high quality, because there are two major problems which must be overcome. The first one is the constitutional supercooling [Singh, Witt, and Gatos (1974); Kim (1978)] which appears in the source solution ahead of the growth interface. When the separation between liquidus and solidus lines is wide, the degree of constitutional supercooling also becomes large, and consequently polycrystals are grown. The second relates to flows caused by heat and mass transfer. The quality of mixed crystals is strongly affected by flow patterns.

Several attempts have been made to reduce the degree of constitutional supercooling and the influence of flow caused by heat and mass transfer. The Czochralski apparatus to rotate a seed crystal with high speeds of 100 to 200 *rpm* [Bachmann, Thiel, Schreiber, and J. (1980)] and accelerated crucible rotation technique [Capper, Gosney, Jones, and Kenworthy (1986)] are the most prominent. We have developed two new methods. One is the Czochralski method modified to introduce ultrasonic vibrational stirring [Hayakawa and Kumagawa (1985)]. $In_xGa_{1-x}Sb$ single crystals with higher In compositional ratio ($0 < x < 0.15$) were grown by using this method [Tsuruta, Hayakawa, and Kumagawa (1988)]. The other method called the rotational Bridgman method (RBM) is similar to the tipping method developed by Nelson (1963) To increase the stirring effect, however, it is different that a relative motion between the growing surface and the solution can be given by rotating the growth ampoule at high speeds, where the growing surface covered about 60 to 90 % with the solution. For the first time, we adopted this method to grow large $InSb_{1-x}Bi_x$, $In_xGa_{1-x}Sb$ and $Ga_{1-x}In_xAs_ySb_{1-y}$ mixed crystals [Ozawa, Hayakawa, and Kumagawa (1991a); Kumagawa, Ozawa, and Hayakawa (1988); Hayakawa, Ozawa, Ando, Koyama, Masaki, Takahashi, and Kumagawa (1996); Ozawa, Hayakawa, Ono, Koyama, and Kumagawa (1997)]. We focused on the relationship between ampoule rotational rate and temperature profile in the growth solution. The model calculated was conformed to an experimental system of InGaSb crystal growth using RBM. This article describes the change of temperature profiles and flow patterns for ampoule rotational rates.
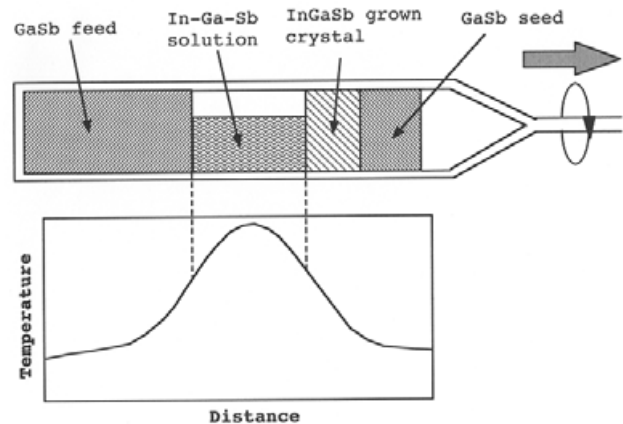
Figure 1 : Schematic representation of the rotational Bridgman method and temperature profile in the furnace.

[1] Shizuoka Institute of Science and Technology, Toyosawa 2200-2, Fukuroi 437-8555, Japan.
[2] Research Institute of Electronics, Shizuoka University, Johoku 3-5-1, Hamamastu 432-8011, Japan

2 Numerical analysis

Fig. 1 shows a schematic RBM growth system and temperature profile in the furnace. In-Ga-Sb solution was put between GaSb seed and feed crystals, where seed and feed crystals were cylindrical in shape, and the In-Ga-Sb solution was semi-cylindrical. Prior to crystal growth, GaSb seed and feed crystals, and primary In-Ga-Sb source materials were charged in the quartz ampoule. The ampoule rotational rates were changed in a range of 0 to 100 *rpm*. Crystal growth was initiated by moving the ampoule toward the low temperature region of the furnace.
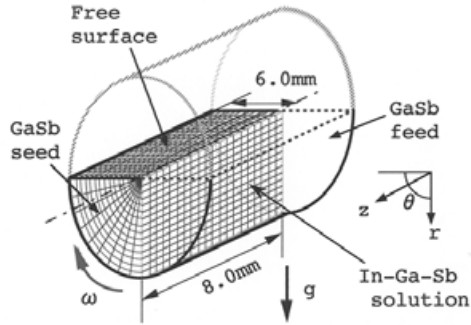
Figure 2 : Three-dimensional model which simulated the experimental system.

Fig. 2 shows a three-dimensional model, which simulated the experimental system, to investigate the relationship between ampoule rotational rate and temperature profile in the solution. This model simulates the In-Ga-Sb solution region in the RBM experimental system in fig.1. The GaSb seed and feed crystals formed in the shape of semicircles were put at the both end of the semi-cylinder. The flat top plate of the semi-cylinder means the free surface of In-Ga-Sb solution. The side wall of the semi-cylinder was the quartz glass wall. The model size is 6 mm in radius and 8 mm long. The In-Ga-Sb solution region consisted of $18 \times 15 \times 20$ segments. r and z were lengths of radial and axial directions of the growth solution reservoir. θ was angle of rotational direction. The flow vector and temperature profile were calculated under a steady state condition. The governing equations are given as follows:

Navier-Stokes equations:

$$\frac{\partial u}{\partial t} + v\frac{\partial u}{\partial r} + \frac{w}{r}\frac{\partial u}{\partial \theta} + u\frac{\partial u}{\partial z} = -\frac{1}{\rho}\frac{\partial p}{\partial z} + \\ v\left(\frac{\partial^2 u}{\partial r^2} + \frac{1}{r}\frac{\partial u}{\partial r} + \frac{1}{r^2}\frac{\partial^2 u}{\partial \theta^2} + \frac{\partial^2 u}{\partial z^2}\right) \quad (1)$$

$$\frac{\partial v}{\partial t} + v\frac{\partial v}{\partial r} + \frac{w}{r}\frac{\partial v}{\partial \theta} + u\frac{\partial v}{\partial z} - \frac{w^2}{r} = -\frac{1}{\rho}\frac{\partial p}{\partial r} + \\ v\left(\frac{\partial^2 v}{\partial r^2} + \frac{1}{r}\frac{\partial v}{\partial r} + \frac{1}{r^2}\frac{\partial^2 v}{\partial \theta^2} + \frac{\partial v}{\partial z} - \frac{v}{r^2} - \frac{2}{r^2}\frac{\partial w}{\partial \theta}\right) + g\beta\Delta T \quad (2)$$

$$\frac{\partial w}{\partial t} + v\frac{\partial w}{\partial r} + \frac{w}{r}\frac{\partial w}{\partial \theta} + u\frac{\partial w}{\partial z} + \frac{vw}{r} = -\frac{1}{\rho}\frac{\partial p}{r\partial \theta} + \\ v\left(\frac{\partial^2 w}{\partial r^2} + \frac{1}{r}\frac{\partial w}{\partial r} + \frac{1}{r^2}\frac{\partial^2 w}{\partial \theta^2} + \frac{2}{r^2}\frac{\partial v}{\partial \theta} - \frac{w}{r^2}\right) \quad (3)$$

Continuity equation:

$$\frac{1}{r}\frac{\partial (vr)}{\partial r} + \frac{1}{r}\frac{\partial w}{\partial \theta} + \frac{\partial u}{\partial z} = 0 \quad (4)$$

Energy equation:

$$\frac{\partial T}{\partial t} + v\frac{\partial T}{\partial r} + \frac{w}{r}\frac{\partial T}{\partial \theta} + u\frac{\partial T}{\partial z} = \\ \alpha\left(\frac{\partial^2 T}{\partial r^2} + \frac{1}{r}\frac{\partial T}{\partial r} + \frac{1}{r^2}\frac{\partial^2 T}{\partial \theta^2} + \frac{\partial^2 T}{\partial z^2}\right) \quad (5)$$

Here r, z and θ are respective coordinate axes in the radial, axial and angular directions. Symbols of u, v, w are axial, radial, and angular flow components of the fluid velocity, α respectively. p the pressure, g the gravitational acceleration, β the volume expansion coefficient, T the temperature, v the kinematic viscosity, α the thermal conductivity.

The following boundary conditions for velocity and temperature were employed. The non-slip condition was applied at the quartz glass wall and the solid-liquid interface.

At the interface between the seed and the solution :

$$u = 0, v = 0, w = \omega(rpm), T = 660(^oC) \quad (6)$$

At the quartz glass wall :

$$u = 0, v = 0, w = \omega(rpm), \quad (7)$$

At the interface between the feed and the solution:

$$u = 0, v = 0, w = \omega(rpm), T = 660(^oC) \quad (8)$$

In the numerical analysis, the rotational rates of growth ampoule were changed in the range of 0 to 100 (*rpm*). The temperature profile ($T(z)$) on the quartz glass wall was determined by measuring the furnace temperature. Flow patterns and temperature profiles were determined by solving the Navier-Stokes (1)-(3), continuity (4), and energy (5) equations. The flow vector and temperature were calculated under a steady state condition. The numerical analysis was performed computationally by the finite differential method.
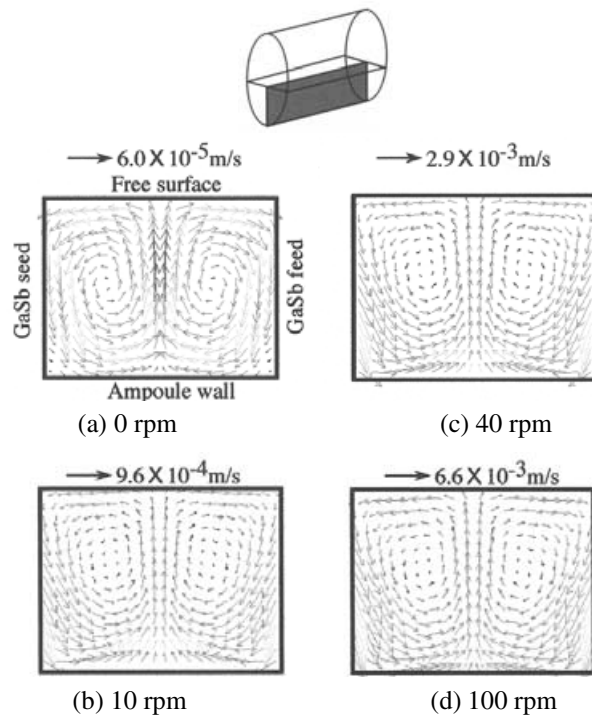
Figure 3 : Flow patterns of Z-R cross section in the In-Ga-Sb solution for the ampoule rotational rates of (a) 0, (b) 10, (c) 40 and (d) 100 *rpm*, respectively.

Figure 4 : Isothermal curves of Z-R cross section in the In-Ga-Sb solution for the ampoule rotational rates of (a) 0, (b) 10, (c) 40 and (d) 100 *rpm*, respectively.

3 Results and discussion

Figs. 3(a)-(d) show flow patterns of Z-R cross section in the In-Ga-Sb solution, where (a), (b), (c) and (d) were calculated under the ampoule rotational rate of 0, 10, 40 and 100 (*rpm*), respectively. In (a), the flow patterns separated into two large flows. One of them, in the left region, moved up the center and down along the GaSb seed wall. The right one flowed symmetrically in the opposite direction. The natural convection generated at the bottom of In-Ga-Sb solution, because the flux heated at the middle of the ampoule wall moved upward the free surface. When the ampoule was not rotated, the fluid flow was only due to the natural convection. In (b), (c) and (d), the flow patterns were basically similar to that of (a). However, centrifugal force due to the rotation of the growth ampoule led to change in fluid flow. The flow velocity became stronger at the side of semi-circle near the interface of seed and feed crystals. The fluid component was concentrated at the center of the solution by centrifugal force, and moved up to the free surface. The flow velocity increased with increasing the ampoule rotational rate. As compared with (a) the result of 0 *rpm*, average flow velocity of 100 *rpm* increased by about one hundred times. As a result, the forced convection brought by the increase of ampoule rotational rate was dominant in the solution.

Figs. 4(a)-(d) illustrate isothermal curves of Z-R cross section in the In-Ga-Sb solution, where the temperature interval was 2^oC. Positions of (a), (b), (c) and (d) correspond to the respective position in Figs. 3. Their curves changed dramatically between ampoule rotational rates of 0 and 100 *rpm*. In (a), the temperature was low at GaSb seed and feed sides and the highest at the center of the ampoule wall. The spacings between isothermal curves became narrow near the interface of the seed and feed crystals. In (b), isothermal curves distributed in wide interval near the center of solution. The results in (c) and (d) also became wide near the interface of the seed and feed crystals. By increasing the ampoule rotational rate, the temperature distribution in the solution became homogeneous.

Figs. 5(a)-(d) show flow patterns(left) and isothermal curves(right) at the interface between the seed and the solution. In the flow pattern of 0 *rpm*, the flux moved down along the GaSb seed wall, because the natural convection occurred at the bottom of In-Ga-Sb solution. In the case of ampoule rotation, a vortex was generated near the center at the solid - liquid interface. The vortex moved in the direction of the arrow, with increasing the ampoule rotational rate. As compared with 0 *rpm*, average flow velocity of 100 *rpm* increased by about one hundred times. Isothermal curves changed dramatically between ampoule rotational rates of 0 and 100 *rpm*. By increasing the ampoule rotational rate, the temperature distri-

(a) 0 rpm

(b) 10 rpm

(c) 40 rpm
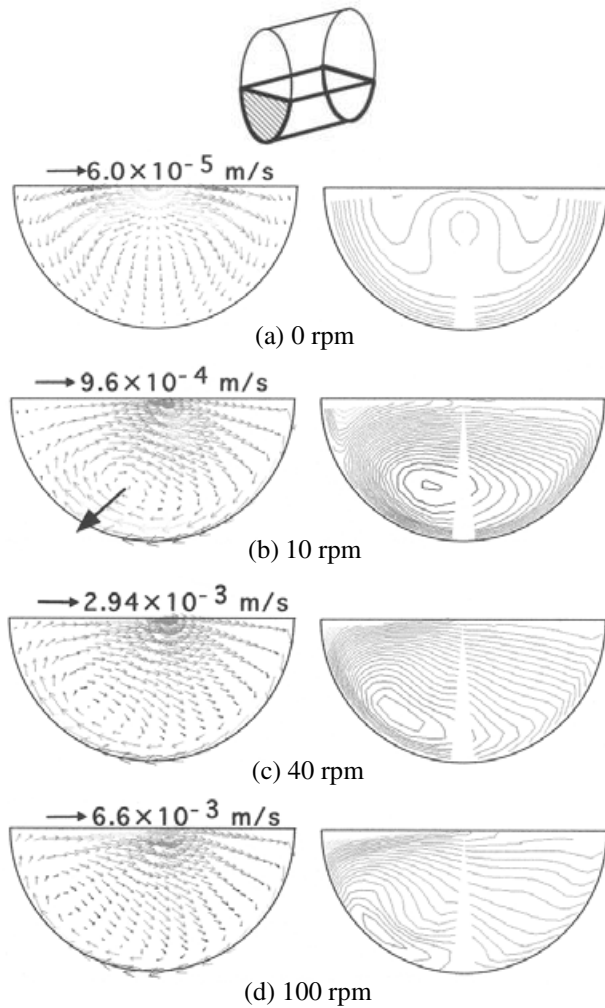
(d) 100 rpm

Figure 5 : Flow patterns and isothermal curves at the interface between the seed and the solution for the ampoule rotational rates of (a) 0, (b) 10, (c) 40 and (d) 100 *rpm*, respectively.

bution in the solution tended to be uniform.

Figs. 6(a)-(d) illustrate isothermal curves of free surfaces in the In-Ga-Sb solution. The curves change dramatically by increasing the ampoule rotational rate from 0 to 100 *rpm*. At 100 *rpm*, the isothermal curves were widely distributed near the center of solution. With increasing the ampoule rotational rate, the temperature distribution became uniform.

Figs. 7(a)-(b) show the relationship between ampoule rotational rate and temperature distribution in the solution, where (a) and (b) were the upper and middle parts of the solution. In (a), the temperature decreased at the center of the solution and increased near seed and feed crystals, with increasing the ampoule rotational rate from 0 to 20 *rpm*. For the ampoule rotational rate greater than 40 *rpm*, the temperature distribution was flat. It was revealed that the stirring effect of ampoule rotation decreased the temperature gradient near the free sur-

face. In (b), the temperature distribution became flater with increasing the ampoule rotational rate. The peak of the temperature distribution was affected by the temperature profile on the ampoule wall. The heights of peak decreased slowly with the ampoule rotation. It is understood that the stirring effect of ampoule rotation, which increased with increasing the rotational rate, affected the mass transfer and heat flux. It is also expected that the ampoule rotation reduces both the degree of constitutional supercooling and the influence of nature convection.

(a) 0 rpm   (c) 40 rpm

(b) 10 rpm   (d) 100 rpm
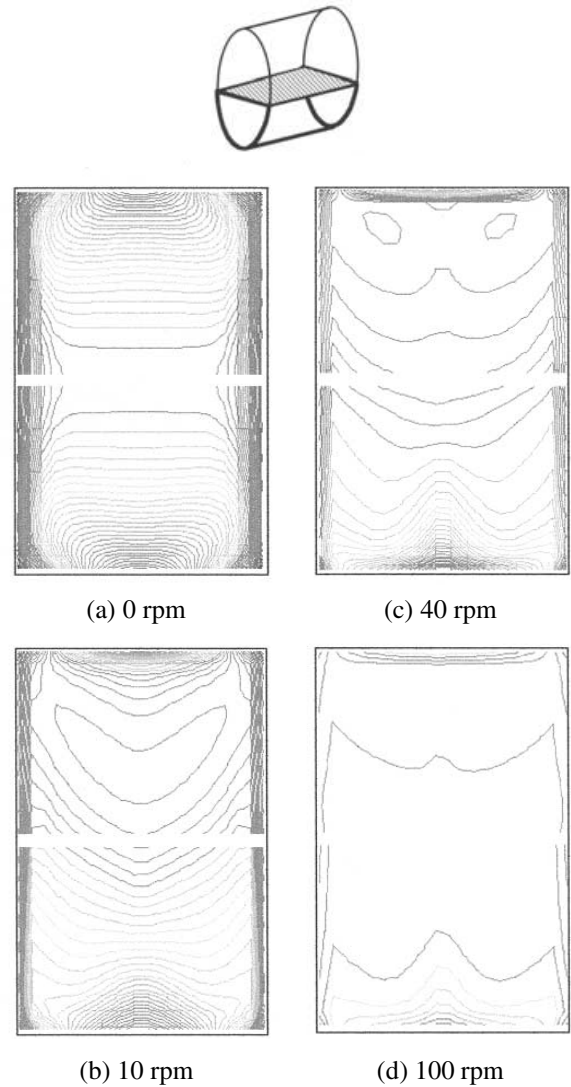
Figure 6 : Isothermal curves of free surface in the In-Ga-Sb solution for the ampoule rotational rates of (a) 0, (b) 10, (c) 40 and (d) 100 *rpm*, respectively.

4   Conclusion

To investigate the solution convection for the rotational Bridgman method, both flow patterns and temperature distributions

(a) Upper part of solution   (b) Middel part of solution
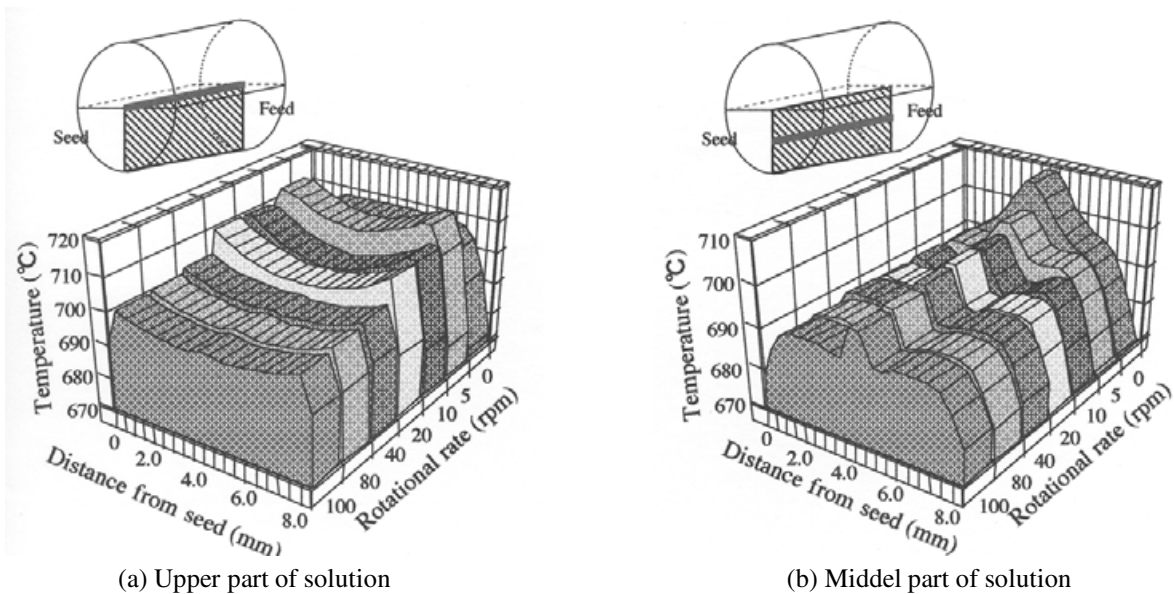
Figure 7 : Relationship between ampoule rotational rates and temperature distribution in the solution, where (a) and (b) were upper and middle parts of the solution.

were calculated by solving three equations in 3-dimensional analysis: Navier-Stokes, continuity and energy. By increasing the ampoule rotational rate from 0 *rpm* to 100 *rpm*, the flow velocity in the In-Ga-Sb solution increased and the temperature distribution became uniform. The stirring effect of ampoule rotation was enhanced with increasing the rotational rate as the forced convection became dominant in the solution.

References

Bachmann, K. J.; Thiel, F. A.; Schreiber, J. H.; J., R. J. (1980): The preparation of Ga-rich GaxIn1-xSb alloy crystals. *J. Electronic Materials*, vol. 9, no. 2, pp. 445–452.

Capper, P.; Gosney, J.; Jones, C. L.; Kenworthy, I. (1986): Bridgman growth of CdxHg1-xTe using ACRT. *J. Electronic Materials*, vol. 15, no. 6, pp. 371–376.

Hayakawa, Y.; Kumagawa, M. (1985): Effect of ultrasonic vibrations on pulled crystals. *Jpn. J. Appl. Phys.*, vol. 24, Suppl.24-1, pp. 166–168.

Hayakawa, Y.; Ozawa, T.; Ando, M.; Koyama, T.; Masaki, M.; Takahashi, K.; Kumagawa, K. (1996): Effect of ampoule rotation on growth of InGaAs ternary bulk crystals from solution. *Cryst. Res. Technol.*, vol. 31, pp. 567–575.

Kim, K. (1978): Morphological instability under constitutional supercooling during the crystal growth of InSb from the melt under stabilizing thermal gradient. *J. Crystal Growth*, vol. 44, pp. 403–413.

Kumagawa, M.; Ozawa, T.; Hayakawa, Y. (1988): A new technique for the growth of III-V mixed crystal layers. *Appl. Surf. Science*, vol. 33/34, pp. 611–618.

Nelson, M. (1963): *RCA Rev.*, pg. 603.

Ozawa, T.; Ando, M.; Hayakawa, Y.; Kumagawa, M. (1996): InGaAs mixed crystals grown by the temperature difference method and the numerical analysis of solution convection. *J. Cryst. Growth*, vol. 166, pp. 463–468.

Ozawa, T.; Hayakawa, Y.; Kumagawa, M. (1991): Growth of III-V ternary and quaternary mixed crystals by the rotationary bridgman method. *J. Crystal Growth*, vol. 109, pp. 212–217.

Ozawa, T.; Hayakawa, Y.; Kumagawa, M. (1991): Interface instability in the growth of Ga1-xInxAsySb1-y and thermodynamic considerations. *J. Cryst. Growth*, vol. 115, pp. 728–732.

Ozawa, T.; Hayakawa, Y.; Ono, H.; Koyama, T.; Kumagawa, M. (1997): Computational analysis of growth rate for InGaAs mixed semiconductors grown by temperature gradient method. In Atluri, S. N.; Yagawa, G.(Eds): *Advances in Computational Engineering Science*, pp. 238–243. Tech Science Press.

Singh, R.; Witt, A. F.; Gatos, H. C. (1974): Oscillatory interface instability during czochralski growth of heavily doped germanium. *J. Electrochem. Soc.*, vol. 121, no. 3, pp. 380–386.

Tsuruta, T.; Hayakawa, Y.; Kumagawa, M. (1988): Effect of ultrasonic vibrations on the growth of InxGa1-xSb mixed crystals. *Jpn. J. Appl. Phys.*, vol. 27, Suppl. 27-1, pp. 47–49.